2011

Predicting shape and stability of air–water interface on superhydrophobic surfaces with randomly distributed, dissimilar posts

B. Emami
Virginia Commonwealth University

Hooman Vahedi Tafreshi
Virginia Commonwealth University, htafreshi@vcu.edu

M. Gad-el-Hak
Virginia Commonwealth University, gadelhak@vcu.edu

Gary C. Tepper
Virginia Commonwealth University, gctepper@vcu.edu

Emami, B., Tafreshi, H.V., Gad-el-Hak, M., et al. Predicting shape and stability of air–water interface on superhydrophobic surfaces with randomly distributed, dissimilar posts. Applied Physics Letters, 98, 203106 (2011).

Predicting shape and stability of air–water interface on superhydrophobic surfaces with randomly distributed, dissimilar posts

B. Emami, H. Vahedi Tafreshi,[a] M. Gad-el-Hak, and G. C. Tepper
Department of Mechanical and Nuclear Engineering, Virginia Commonwealth University, Richmond, Virginia 23284-3015, USA

(Received 28 March 2011; accepted 20 April 2011; published online 19 May 2011)

A mathematical framework developed to calculate the shape of the air–water interface and predict the stability of a microfabricated superhydrophobic surface with randomly distributed posts of dissimilar diameters and heights is presented. Using the Young–Laplace equation, a second-order partial differential equation is derived and solved numerically to obtain the shape of the interface, and to predict the critical hydrostatic pressure at which the superhydrophobicity vanishes in a submersed surface. Two examples are given for demonstration of the method's capabilities and accuracy. © *2011 American Institute of Physics*. [doi:10.1063/1.3590268]

A combination of hydrophobicity and microfabricated roughness can result in a phenomenon known as superhydrophobicity. The drag force imparted by a moving liquid in contact with a superhydrophobic surface is reduced because the air entrapped inside the pores of the surface reduces the contact between water and solid walls.[1] Superhydrophobic surfaces can, therefore, be exploited to reduce the drag force exerted on submerged moving objects such as ships, submarines, or torpedoes. Superhydrophobic surfaces are often manufactured by microfabrication of grooves or posts on a hydrophobic surface. When the pore space on a superhydrophobic surface is filled with air, the system is considered to be at the Cassie state.[2] If the hydrostatic pressure is high, water may penetrate into the pores of the surface and replace the air. This results in the elimination of superhydrophobicity, and transition to the so called Wenzel state.[3,4] The pressure at which a superhydrophobic surface departs from the Cassie state, and therefore the superhydrophobic property vanishes, is referred to as the critical pressure in this work.

Balance of forces has previously been used to study the meniscus shape in capillary tubes,[5,6] capillary channels,[7] shape of a droplet,[8–12] and liquid bridge that forms when a solid disk is withdrawn from a liquid reservoir,[13] as well as the capillary rise between vertical plates.[14] Only a few studies have applied balance of forces to investigate the shape and stability of the air–water menisci of superhydrophobic surfaces. Extrand[15,16] applied balance of forces to a superhydrophobic surface with ordered pillars to study the stability of the meniscus formed by a drop on the surface. By applying balance of forces, an analytical relationship was proposed by Zheng *et al.*[17] to predict the stability of the meniscus formed between the cylindrical posts or square pillars on a microfabricated superhydrophobic surface.

In the present work, we developed a method to calculate the meniscus shape under different hydrostatic pressures of any microfabricated superhydrophobic surface with randomly distributed circular posts of dissimilar diameters, heights, and materials. The shape of the meniscus is then used to calculate the critical hydrostatic pressure at which the superhydrophobicity of the surface vanishes. Note that the existing models can only be applied to surfaces with orderly distributed identical posts. Beyond the microfabricated superhydrophobic surfaces, the present method can potentially be used to calculate the critical pressure of surfaces with fibrous superhydrophobic coatings.[18,19]

Consider a superhydrophobic surface with a set of identical posts orderly placed next to one another. Figure 1(a) shows a schematic of a post and the corresponding meniscus; d, h, and L represent the post diameter, height, and the center to center distance between two neighboring posts, respectively. Note that because of the geometrical symmetry, only

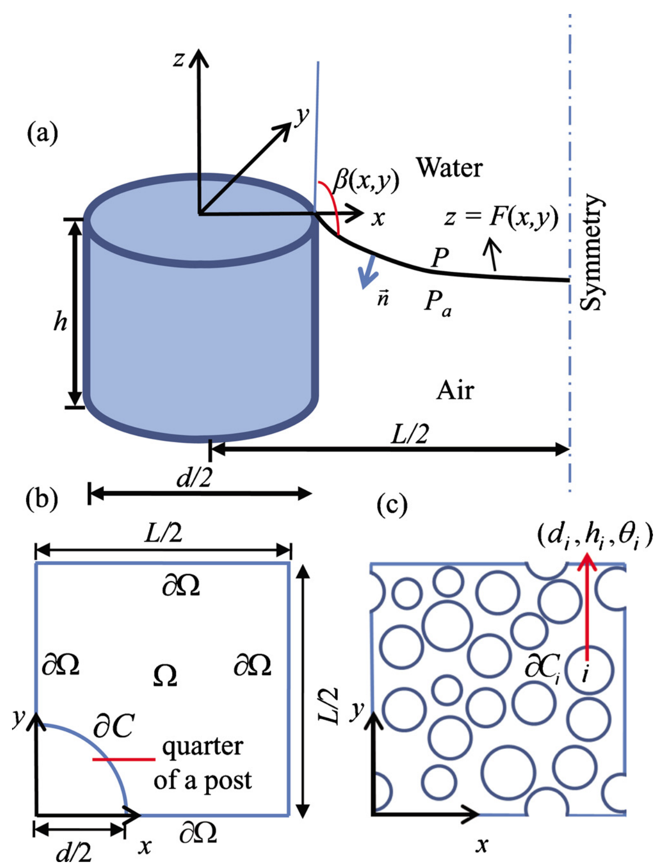

FIG. 1. (Color online) Schematic of (a) a post with the corresponding air–water meniscus; (b) computational domain for a surface with ordered identical posts; and (c) computational domain for a general surface with randomly distributed dissimilar posts.

[a]Electronic mail: htafreshi@vcu.edu.

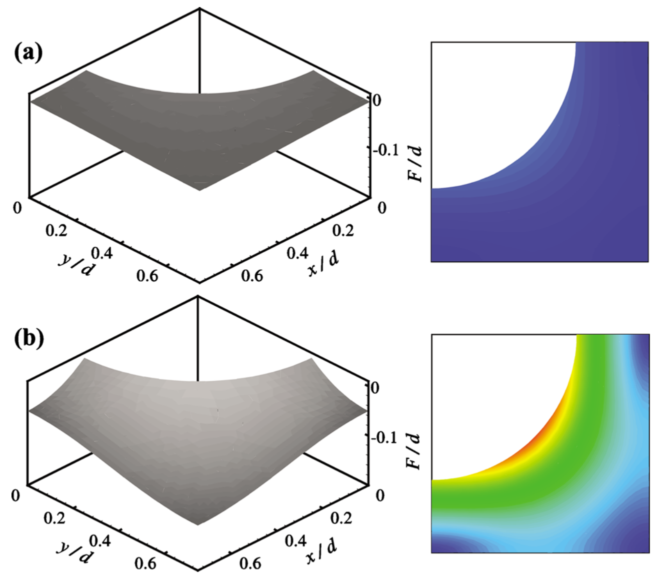

FIG. 2. (Color online) Calculated meniscus surfaces and gradient ($|\nabla F|$) contours for a superhydrophobic surface with ordered identical posts at (a) $P=1000$ and (b) $P=7000$ Pa. The contour values are in the range of 0 to 0.6 (blue to red in the online version). Note that due to symmetry, the results correspond to a quarter of one post.

half of the meniscus is shown. A Cartesian coordinate system is chosen such that the z-axis is along the symmetry axis of the post, and the coordinates' origin is on the top of the post. By applying balance of forces on the meniscus $z=F(x,y)$ one gets

$$P + P_\infty - P_a - \sigma \nabla \cdot \vec{n} = 0, \tag{1}$$

where P is the gauge hydrostatic pressure, P_∞ is the ambient pressure, P_a is the pressure in the entrapped air, σ is the air–water surface tension, and $\vec{n}$ is the surface unit normal vector. Here, it is assumed that $P \gg \rho g|F|$, and so the pressure is uniform over the meniscus. Let us define a function $G(x,y,z) \equiv F(x,y) - z$. Obviously, $G(x,y,z)=0$ on the meniscus surface. It can be shown that the meniscus surface unit normal vector, $\vec{n}$, can be calculated as a function of G as $\vec{n}=\nabla G/|\nabla G|$. Hence, $n_x=(1+F_x^2+F_y^2)^{-1/2}F_x$, $n_y=(1+F_x^2+F_y^2)^{-1/2}F_y$, and $n_z=-(1+F_x^2+F_y^2)^{-1/2}$, where n_x, n_y, and n_z are the components of $\vec{n}$ in x, y, and z directions, respectively, and $F_x=\partial F/\partial x$, and $F_y=\partial F/\partial y$.

Assuming that $h \gg |F|$, the pressure of the entrapped air is not affected by the meniscus shape, and therefore, $P_a \approx P_\infty$. Equation (1) then reduces to $\nabla \cdot \vec{n}=\xi$, where $\xi=P/\sigma$. One gets

$$(1 + F_y^2)F_{xx} + (1 + F_x^2)F_{yy} - 2F_xF_yF_{xy} = \xi(1 + F_x^2 + F_y^2)^{3/2}, \tag{2}$$

where indices x and y represent the partial derivatives with respect to x and y, respectively. This yields a second-order nonlinear partial differential equation (PDE) which is solved numerically. Due to symmetry, the equation is solved in a domain representing a quarter of one post, as shown in Fig. 1(b). Note that Ω represents the whole domain, ∂C represent the domain boundary at the post wall, and $\partial\Omega$ represents all other boundaries. Equation (1) is subject to the boundary conditions $F|_{\partial C}=0$ and $\partial F/\partial n|_{\partial\Omega}=0$.

Using the computed water–air interface surface, $z=F(x,y)$, one can calculate the critical hydrostatic pressure at which the superhydrophobicity fails. It is known that the failure occurs when the angle between the meniscus and post, $\beta(x,y)$, reaches the water–air–solid flat surface contact angle.[15–17] Hence, the superhydrophobicity is dependent upon the condition $\beta(x,y) < \theta$, where θ is the water–air–solid flat surface contact angle. Therefore, unless the condition

$$|\nabla F|_{\partial C} < |\cot \theta| \tag{3}$$

holds on a surface with ordered circular posts, the superhydrophobicity fails.

The above formulation is valid for any superhydrophobic surface with randomly distributed circular posts of different diameters, materials, and heights. Figure 1(c) shows a computational domain with randomly distributed posts. Each post i has a diameter d_i and a height h_i, and is of a material with a flat surface contact angle θ_i. A boundary condition $F|_{\partial C_i}=h_i-\max\{h_j\}$ is applied on the post walls, $\{\partial C_j\}$, and so $F=0$ on the boundary of the tallest post. With the randomly distributed posts, periodic boundary condition is applied on all other boundaries, $\partial\Omega$. In the same way, the above condition can be generalized as

$$\forall i{:}|\nabla F|_{\partial C_i} < |\cot \theta_i|. \tag{4}$$

We used the FLEXPDE program from PDESolutions Inc. to solve Eq. (2), along with the above boundary conditions. All the numerical solutions were run on a workstation with a dual core 2.4 GHz CPU, and 4 GB of RAM; each solution took less than a minute. Careful attention was paid to ensure that the results of our calculations are not dependent on the choice of the mesh size.

Unlike the work of Zheng *et al.*[17] who assumed that the meniscus slope does not change along the perimeter of a post, which is an oversimplification considering the lack of axisymmetry in an ordered post configuration, our model allows the slope to adapt itself along a post perimeter based on the relative positions of the neighboring posts.

For validation purposes, we applied our method to a microfabricated surface with circular posts with a diameter of $d=10$ μm orderly located next to each other, with a center to center distance of $L=1.5d$, corresponding to a gas area fraction of 65%. Here we assume that posts have identical heights. The posts are made up of a hydrophobic material with a water–solid contact angle of 120°. Equation (2) was solved in a computational domain similar to what was shown in Fig. 1(b). Figures 2(a) and 2(b) show the results for the meniscus surface, $F(x,y)$, at hydrostatic pressures of 1000 Pa and 7000 Pa, respectively. The surface function F, and the coordinates x and y are normalized with the post diameter. It can be seen that the meniscus curves and dips under the hydrostatic pressure, and that the curvature and the dip increase with pressure. At a hydrostatic pressure of 7000 Pa, the depth of the meniscus is significant, and reaches about 20% of the post diameter at the deepest point. Equation (3) was then used to calculate the critical pressure. Figures 2(a) and 2(b) also show the contours for the value of the meniscus surface gradient, $|\nabla F|$ at the above pressures. As one would expect, the maximum surface gradient occurs in the vicinity of the post wall, where the meniscus slope is maximum. Furthermore, the meniscus gradient increases with hydrostatic pressure. The surface remains superhydrophobic, if $|\nabla F|$ is less than $|\cot \theta|=|\cot 120°| \approx 0.58$. At a hydrostatic

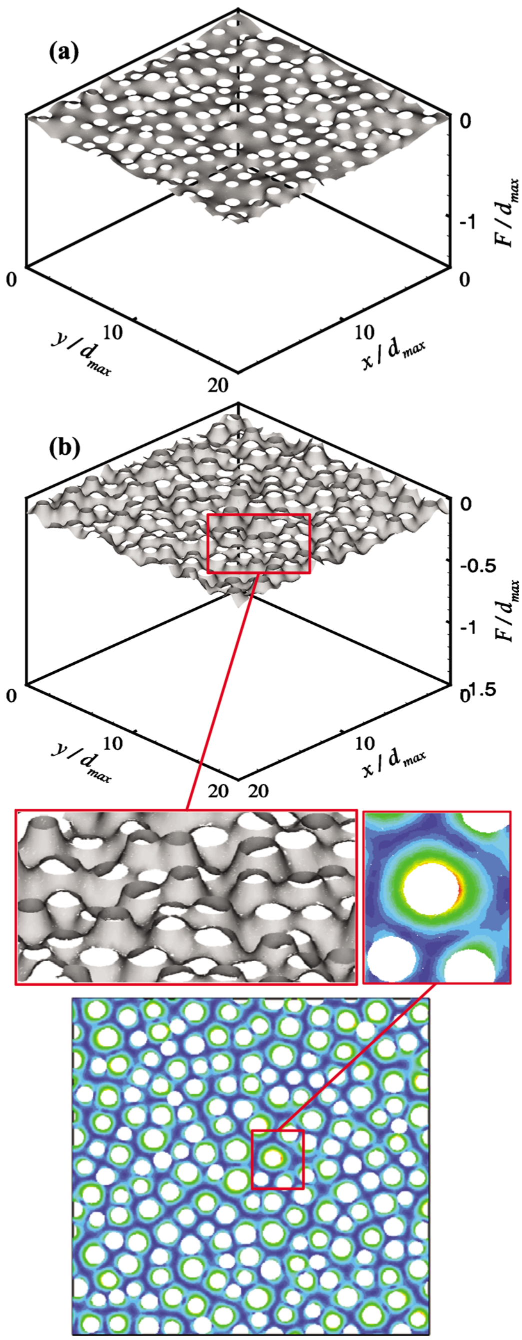

FIG. 3. (Color online) Calculated meniscus surfaces and gradient ($|\nabla F|$) contours for a superhydrophobic surface with randomly distributed posts of random diameters and heights at (a) $P=100$ and (b) $P=3400$ Pa. The contour values are in the range of 0 to 0.6 (blue to red in the online version). The zoomed in illustrations are provided for a better visualization, and correspond to the location where the superhydrophobicity starts to vanish.

pressure of 7000 Pa, the value of the meniscus gradient approaches 0.58 in the vicinity of the post. More precisely, our calculations revealed that Eq. (3) does not hold beyond a hydrostatic pressure of 7200 Pa, i.e., the critical pressure. It is worth mentioning that the model of Zheng *et al.*[17] predicts a critical pressure of 7800 Pa for the surface considered here. As mentioned earlier, we believe that our model is more accurate, as it calculates the local slope of the meniscus on the post perimeter with no simplifying assumptions.

To demonstrate capabilities of our method, we calculated the meniscus shape and the critical pressure for a superhydrophobic surface with randomly distributed posts of dissimilar diameters ranging between 8 and 12 μm, and random heights ranging between 50 and 51 μm. The surface gas area fraction and the flat surface contact angle were 65% and 120°, respectively. Figures 3(a) and 3(b) present the predicted meniscus surfaces, at the hydrostatic pressures of 100 Pa and 3400 Pa, respectively. Again, the results show that the depth of the meniscus shape, and therefore the value of the meniscus gradient, increases with pressure (see the contours of meniscus gradient). Again, the maximum meniscus gradient occurs in the vicinity of the posts, and increases with hydrostatic pressure. At a pressure of 3400 Pa the maximum value of the meniscus gradient approaches $0.58(=|\cot\theta| = |\cot 120°|)$, and so the superhydrophobicity starts to vanish. Note that the critical pressure of the surface with randomly distributed posts of dissimilar heights and diameters is much lower than that of a similar surface with ordered identical post, as expected.[20]

In summary, we have developed a general method to calculate the meniscus shape and the critical pressure of any superhydrophobic surface with randomly distributed circular posts of dissimilar diameters, heights, and materials. We believe that this method is more accurate than any previously developed method and is computationally inexpensive.

Financial support from the Defense Advanced Research Projects Agency (DARPA), Contract No. W91CRB-10-1-0003, is acknowledged.

[1] J. Wang, F. Liu, H. Chen, and D. Chen, Appl. Phys. Lett. **95**, 084104 (2009).
[2] A. B. D. Cassie and S. Baxter, Trans. Faraday Soc. **40**, 546 (1944).
[3] R. N. Wenzel, Ind. Eng. Chem. **28**, 988 (1936).
[4] J. P. Rothstein, Annu. Rev. Fluid Mech. **42**, 89 (2010).
[5] D. Siegel, Pac. J. Math. **88**, 471 (1980).
[6] R. Finn, Z. Angew. Math. Mech. **61**, 165 (1981).
[7] R. López, Nonlinearity **20**, 1573 (2007).
[8] S. Levine, J. Lowndes, E. J. Watson, and G. Neale, J. Colloid Interface Sci. **73**, 136 (1980).
[9] R. Finn, Pac. J. Math. **88**, 541 (1980).
[10] A. S. Dimitrov, P. A. Kravchelsky, A. D. Nikolov, H. Noshi, and M. Matsumoto, J. Colloid Interface Sci. **145**, 279 (1991).
[11] J. Graham-Eagle and S. Pennell, Int. J. Numer. Methods Fluids **32**, 851 (2000).
[12] L. R. White, J. Colloid Interface Sci. **258**, 82 (2003).
[13] T. I. Vogel, Pac. J. Math. **103**, 205 (1982).
[14] F. J. Higuera, A. Medina, and A. Linan, Phys. Fluids **20**, 102102 (2008).
[15] C. W. Extrand, Langmuir **18**, 7991 (2002).
[16] C. W. Extrand, Langmuir **20**, 5013 (2004).
[17] Q. S. Zheng, Y. Yu, and Z. H. Zhao, Langmuir **21**, 12207 (2005).
[18] M. A. Samaha, F. O. Ochanda, H. V. Tafreshi, G. C. Tepper, and M. Gad-el-Hak, Rev. Sci. Instrum. **82**, 045109 (2011).
[19] Z. Jia, M. Liu, F. Liu, Y. Luo, D. Jia, and B. Guo, Appl. Phys. Lett. **96**, 043108 (2010).
[20] M. A. Samaha, H. V. Tafreshi, and M. Gad-el-Hak, Phys. Fluids **23**, 012001 (2011).